multiplied by R, the classical electron radius, they become entirely equivalent to the corresponding quantities in neutron usage, which are lengths. It should be noted that the presence of different isotopes and the effect of nuclear spin (disordered except under very special conditions) give rise to incoherent elastic neutron scattering, which has no equivalent in the X-ray case. The scattering length corresponding to R times the atomic scattering factor for X-rays is therefore the coherent scattering length, $b_{\rm coh}$, obtained by averaging the scattering length over the nuclear spin state and isotope distribution.

5.3.2.3. *Absorption*

Neutron absorption is related to a nuclear reaction in which the neutron combines with the absorbing nucleus to form a compound nucleus, usually in a metastable state which then decays. The scattering length describing this resonance scattering process depends on the neutron energy and contains an imaginary part associated with absorption in complete analogy with the imaginary part of the dispersion correction for the X-ray atomic scattering factors. The energies of the resonances are usually far above those of interest for crystallography, and the linear absorption coefficient varies approximately as $1/v$ or λ. It is important to note that, except for a very few cases (notably ^{3}He, ^{6}Li, ^{10}B, In, Cd, Gd), the absorption of neutrons is very small compared with that of X-rays, and even more so compared with that of electrons, and can be neglected to a first approximation.

5.3.2.4. *Differences between neutron and X-ray scattering*

There are major differences in the experimental aspects of neutron and X-ray scattering. Neutrons are only available in large facilities, where allocation of beam time to users is made on the basis of applications, and where admittance is restricted because of the hazards which nuclear technology can present in the hands of ill-intentioned users. Because of the radiation shielding necessary, as well as the large size of neutron detectors, neutron-scattering instrumentation is much bulkier than that for X-rays. Neutron beams are in some aspects similar to synchrotron radiation, in particular because in both cases the beams are initially 'white' and for most applications have to be monochromated. There is, however, a huge difference in the order of magnitudes of the intensities. Neutron beams are weak in comparison with laboratory X-ray sources, and weaker by many orders of magnitude than synchrotron radiation. Also, the beam sources are large in the case of neutrons, since they are essentially the moderators, whereas the source is very small in the case of synchrotron radiation, and this difference again increases the ratio of the brilliances in favour of X-rays. This encourages the use of large specimens in all neutron-scattering work, and makes the extinction problem more important than for X-rays. Furthermore, many experiments that are quick using X-rays become very slow, and give rise to impaired resolution, in the neutron case.

There are also at least two additional aspects of neutron scattering in comparison with X-ray scattering, apart from the effect of the magnetic moment associated with the intrinsic (spin) angular momentum of the neutron. On the one hand, the small velocity of neutrons, compared with the velocity of light, makes time-of-flight measurements possible, both in standard neutron diffraction and in investigations of perfect crystals. Because this velocity is of the same order of magnitude as that of ultrasound, the effect of ultrasonic excitation on neutron diffraction is slightly different from that in the X-ray case. On the other hand, the fact that neutrons have mass and a magnetic moment implies that they can be affected by external fields, such as gravity and magnetic fields, both during their propagation in air or in a vacuum and while being diffracted within crystals (Werner, 1980) (see Section 5.3.5). Experiments completely different from the X-ray case can thus be performed with perfect crystals and with neutron interferometers (see Sections 5.3.6 and 5.3.7.3).

5.3.2.5. *Translating X-ray dynamical theory into the neutron case*

As shown in Chapter 5.1, the basic equations of dynamical theory, *viz* Maxwell's equations for the X-ray case and the time-independent Schrödinger equation in the neutron case, have exactly the same form when the effect of the neutron spin can be neglected, *i.e.* in situations that do not involve magnetism and when no externally applied potential is taken into account. The translation scheme for the scattering factors and structure factors is described above. The one formal difference is that the wavefunction is scalar in the neutron case, hence there is no equivalent to the parallel and perpendicular polarizations of the X-ray situation: C in equation (5.1.2.20) of Chapter 5.1 should therefore be set to 1.

The physics of neutron diffraction by perfect crystals is therefore expected to be very similar to that of X-ray diffraction, with the existence of wavefields, *Pendellösung* effects, anomalous transmission, intrinsic rocking-curve shapes and reflectivity *versus* thickness behaviour in direct correspondence. All experimental tests of these predictions confirm this view (Section 5.3.6).

Basic discussions of dynamical neutron scattering are given by Stassis & Oberteuffer (1974), Sears (1978), Rauch & Petrascheck (1978), and Squires (1978).

5.3.3. Neutron spin, and diffraction by perfect magnetic crystals

5.3.3.1. *Polarization of a neutron beam and the Larmor precession in a uniform magnetic field*

A polarized neutron beam is represented by a two-component spinor,

$$|\varphi\rangle = \begin{pmatrix} c \\ d \end{pmatrix} = c\begin{pmatrix} 1 \\ 0 \end{pmatrix} + d\begin{pmatrix} 0 \\ 1 \end{pmatrix},$$

which is the coherent superposition of two states, of different amplitudes c and d, polarized in opposite directions along the spin-quantization axis. The spinor components c and d are generally space- and time-dependent. We suppose that $\langle\varphi|\varphi\rangle = cc^* + dd^* = 1$. The polarization vector $\mathbf{P}$ is defined as

$$\mathbf{P} = \langle\varphi|\boldsymbol{\sigma}|\varphi\rangle,$$

where the vector $\boldsymbol{\sigma}$ represents the set of Pauli matrices σ_x, σ_y and σ_z. The components of $\mathbf{P}$ are

$$\begin{aligned} P_x &= (\,c^* \quad d^*\,)\sigma_x\begin{pmatrix} c \\ d \end{pmatrix} = (\,c^* \quad d^*\,)\begin{pmatrix} 0 & 1 \\ 1 & 0 \end{pmatrix}\begin{pmatrix} c \\ d \end{pmatrix} \\ &= c^*d + cd^* \\ P_y &= (\,c^* \quad d^*\,)\sigma_y\begin{pmatrix} c \\ d \end{pmatrix} = (\,c^* \quad d^*\,)\begin{pmatrix} 0 & -i \\ i & 0 \end{pmatrix}\begin{pmatrix} c \\ d \end{pmatrix} \\ &= i(cd^* - c^*d) \\ P_z &= (\,c^* \quad d^*\,)\sigma_z\begin{pmatrix} c \\ d \end{pmatrix} = (\,c^* \quad d^*\,)\begin{pmatrix} 1 & 0 \\ 0 & -1 \end{pmatrix}\begin{pmatrix} c \\ d \end{pmatrix} \\ &= cc^* - dd^*, \end{aligned} \tag{5.3.3.1}$$

from which it is clearly seen that, unlike P_z, the polarization components P_x and P_y depend on the phase difference between the spinor components c and d.

In a region of a vacuum in which a uniform magnetic field **B** is present, a neutron beam experiences a magnetic potential energy represented by the matrix

$$-\mu_n \boldsymbol{\sigma} \cdot \mathbf{B} = \begin{pmatrix} -\mu_n B & 0 \\ 0 & \mu_n B \end{pmatrix},$$

μ_n being the neutron magnetic moment, if the directions of **B** and of the spin-quantization axis coincide. Consequently, different indices of refraction $n = 1 \pm (\mu_n B/2E)$, where E is the neutron energy, should be associated with the spinor components c and d; this induces between these spinor components a phase difference which is a linear function of the time (or, equivalently, of the distance travelled by the neutrons), hence, according to (5.3.3.1), a rotation around the magnetic field of the component of the neutron polarization perpendicular to this magnetic field. The time frequency of this so-called Larmor precession is $2\mu_n B/h$, where h is Planck's constant.

A neutron beam may be partially polarized; such a beam is conveniently represented by a spin-density matrix ρ, which is the statistical average of the spin-density matrices associated to the polarized beams which are mixed incoherently, the density matrix associated to the spinor

$$|\varphi\rangle = \begin{pmatrix} c \\ d \end{pmatrix}$$

being

$$|\varphi\rangle\langle\varphi| = \begin{pmatrix} c \\ d \end{pmatrix}(c^* \quad d^*) = \begin{pmatrix} cc^* & cd^* \\ c^*d & dd^* \end{pmatrix}.$$

The polarization vector **P** is then obtained as

$$\mathbf{P} = \mathrm{Tr}(\boldsymbol{\sigma}\rho). \tag{5.3.3.2}$$

In the common case of a non-polarized beam, the spin-density matrix is

$$\rho = \frac{1}{2}\begin{pmatrix} 1 & 0 \\ 0 & 1 \end{pmatrix}.$$

It is easily seen that all components of **P** are then equal to 0.

Equation (5.3.3.2) is therefore applicable to the general case (polarized, partially polarized or non-polarized beam). The inverse relation giving the density matrix ρ as function of **P** is

$$\rho = \frac{1}{2}\begin{pmatrix} 1 & 0 \\ 0 & 1 \end{pmatrix} + \frac{1}{2}\mathbf{P} \cdot \boldsymbol{\sigma}. \tag{5.3.3.3}$$

5.3.3.2. *Magnetic scattering by a single ion having unpaired electrons*

The spin and orbital motion of unpaired electrons in an atom or ion give rise to a surrounding magnetic field $\mathbf{B}(\mathbf{r})$ which acts on the neutron *via* the magnetic potential energy $-\boldsymbol{\mu}_n \cdot \mathbf{B}(\mathbf{r})$, where $\boldsymbol{\mu}_n$ is the neutron magnetic moment. Since this is a long-range interaction, in contrast to the nuclear interaction, the magnetic scattering length p, which is proportional to the Fourier transform of the magnetic potential energy distribution $-\boldsymbol{\mu}_n \cdot \mathbf{B}(\mathbf{r})$, depends on the angle of scattering.

The classical relation $\mathrm{div}\, \mathbf{B}(\mathbf{r}) = 0$ shows clearly that the vector $\mathbf{B}(\mathbf{s})$, which is the Fourier transform of $\mathbf{B}(\mathbf{r})$, is perpendicular to the reciprocal-space vector **s**. If we consider the magnetic field $\mathbf{B}(\mathbf{r})$ as resulting from a point-like magnetic moment $\boldsymbol{\mu}$ at position $\mathbf{r} = 0$, we get

$$\mathbf{B}(\mathbf{r}) = \frac{\mu_0}{4\pi}\mathrm{curl}\frac{\boldsymbol{\mu} \times \mathbf{r}}{r^3},$$

where $\mu_0 = 4\pi \times 10^{-7}$ H m^{-1} is the permittivity of a vacuum and $\times$ denotes the cross product. $\mathbf{B}(\mathbf{r})$ can be Fourier-transformed into

$$\mathbf{B}(\mathbf{s}) = \mu_0 \mathbf{s} \times \frac{\boldsymbol{\mu} \times \mathbf{s}}{s^2} = \mu_0 \boldsymbol{\mu}_\perp(\mathbf{s}), \tag{5.3.3.4}$$

where $\boldsymbol{\mu}_\perp(\mathbf{s})$ is the projection of $\boldsymbol{\mu}$ on the plane perpendicular to **s** (reflecting plane).

This result can be applied by volume integration to the more general case of a spatially extended magnetization distribution, which for a single magnetic ion corresponds to the atomic shell of the unpaired electrons. It is thus shown that the magnetic scattering length is proportional to $\boldsymbol{\mu}_n \cdot \boldsymbol{\mu}_{i\perp}$, where $\boldsymbol{\mu}_{i\perp}$ is the projection of the magnetic moment of the ion on the reflecting plane.

For a complete description of magnetic scattering, which involves the spin-polarization properties of the scattered beam, it is necessary to represent the neutron wavefunction in the form of a two-component spinor and the ion's magnetic moment as a spin operator which is a matrix expressed in terms of the Pauli matrices $\boldsymbol{\sigma}$ $(\sigma_x, \sigma_y, \sigma_z)$. The magnetic scattering length is therefore itself a (2×2) matrix:

$$(\mathrm{p}) = -(2\pi m/h^2)\mu_n \boldsymbol{\sigma} \cdot \mathbf{B}(\mathbf{s}) = -\mu_0 (2\pi m/h^2)\mu_n \boldsymbol{\sigma} \cdot \boldsymbol{\mu}_{i\perp}(\mathbf{s}) f_i(\sin\theta/\lambda), \tag{5.3.3.5}$$

where $f_i(\sin\theta/\lambda)$ is the dimensionless magnetic form factor of the ion considered and tends towards a maximum value of 1 when the scattering angle θ tends towards 0 (forward scattering). The value of $\mu_0(2\pi m/h^2)\mu_n\mu_i$ is $p_1 = 2.70 \times 10^{-15}$ m for $\mu_i = 1$ Bohr magneton.

According to (5.3.3.4) or (5.3.3.5), there is no magnetic scattering in directions such that the scattering vector **s** is in the same direction as the ion magnetic moment $\boldsymbol{\mu}_i$. Magnetic scattering effects are maximum when **s** and $\boldsymbol{\mu}_i$ are perpendicular.

The matrix (p) is diagonal if the direction of $\boldsymbol{\mu}_{i\perp}(\mathbf{s})$ is chosen as the spin-quantization axis. Therefore, there is no spin-flip scattering if the incident beam is polarized parallel or antiparallel to the direction of $\boldsymbol{\mu}_{i\perp}(\mathbf{s})$.

It is more usual to choose the spin-quantization axis (Oz) along $\boldsymbol{\mu}_i$. Let β be the angle between the vectors $\boldsymbol{\mu}_i$ and **s**; the (x, y, z) components of $\boldsymbol{\mu}_{i\perp}(\mathbf{s})$ are then $(-\mu_i \sin\beta\cos\beta, 0, \mu_i \sin^2\beta)$ if the y axis is chosen along $\boldsymbol{\mu}_i \times \mathbf{s}$. The total scattering length, which is the sum of the nuclear and the magnetic scattering lengths, is then represented by the matrix

$$(\mathrm{q}) = \begin{pmatrix} b + p\sin^2\beta & -p\sin\beta\cos\beta \\ -p\sin\beta\cos\beta & b - p\sin^2\beta \end{pmatrix}, \tag{5.3.3.6}$$

where b is the nuclear scattering length and

$$p = -\mu_0 \frac{2\pi m}{h^2}\mu_n \mu_i f_i\left(\frac{\sin\theta}{\lambda}\right) = -p_1 \mu_i f_i\left(\frac{\sin\theta}{\lambda}\right),$$

with μ_i expressed in Bohr magnetons. The relations

$$(\mathrm{q})\begin{pmatrix} 1 \\ 0 \end{pmatrix} = \begin{pmatrix} b + p\sin^2\beta \\ -p\sin\beta\cos\beta \end{pmatrix} \text{ and}$$

$$(\mathrm{q})\begin{pmatrix} 0 \\ 1 \end{pmatrix} = \begin{pmatrix} -p\sin\beta\cos\beta \\ b - p\sin^2\beta \end{pmatrix}$$

show clearly that the diagonal and the non-diagonal elements of the matrix (q) are, respectively, the spin-flip and the non-spin-flip scattering lengths. It is usual to consider the scattering cross sections, which are the measurable quantities. The cross sections for neutrons polarized parallel or antiparallel to the ion magnetic moment are

$$(\mathrm{d}\sigma/\mathrm{d}\Omega)_\pm = b^2 \pm 2bp\sin^2\beta + (p\sin\beta)^2. \tag{5.3.3.7}$$

These expressions are the sum of the spin-flip and non-spin-flip cross sections, which are equal to $(b \pm p \sin^2\beta)^2$ and $(p \sin\beta \cos\beta)^2$, respectively. In the case of non-polarized neutrons, the interference term $(\pm 2bp \sin^2\beta)$ between the nuclear and the magnetic scattering disappears; the cross section is then

$$(\mathrm{d}\sigma/\mathrm{d}\Omega) = b^2 + (p \sin\beta)^2. \qquad (5.3.3.8)$$

In the general case of a partially polarized beam we can use the density-matrix representation. Let ρ_{inc} be the density matrix of the incident beam; it can be shown that the density matrix of the diffracted beam is equal to the following product of matrices: $(\mathrm{q})\rho_{\mathrm{inc}}(\mathrm{q}^*)$. Using the relations between the density matrix and polarization vector presented in the preceding section, we can obtain a general description of the diffracted beam as a function of the polarization properties of the incident beam. Such a formalism is of interest for dealing with new experimental arrangements, in which a three-dimensional polarization analysis of the diffracted beam is possible, as shown by Tasset (1989).

5.3.3.3. *Dynamical theory in the case of perfect ferromagnetic or collinear ferrimagnetic crystals*

The most direct way to develop this dynamical theory in the two-beam case, which involves a single Bragg-diffracted beam of diffraction vector **h**, is to consider spinor wavefunctions of the following form:

$$\varphi(\mathbf{r}) = \exp(i\mathbf{K_0}\cdot\mathbf{r})\begin{pmatrix} D_0 \\ E_0 \end{pmatrix} + \exp[i(\mathbf{K_0}+\mathbf{h})\mathbf{r}]\begin{pmatrix} D_h \\ E_h \end{pmatrix} \qquad (5.3.3.9)$$

as approximate solutions of the wave equation inside the crystal,

$$\Delta\varphi(\mathbf{r}) + k^2\varphi(\mathbf{r}) = [u(\mathbf{r}) - \boldsymbol{\sigma}\cdot\mathbf{Q}(\mathbf{r})]\varphi(\mathbf{r}), \qquad (5.3.3.10)$$

where $u(\mathbf{r})$ and $-\boldsymbol{\sigma}\cdot\mathbf{Q}(\mathbf{r})$ are, respectively, equal to the nuclear and the magnetic potential energies multiplied by $2m/\hbar^2$. In the calculation of $\varphi(\mathbf{r})$ in the two-beam case, we need only three terms in the expansions of the functions $u(\mathbf{r})$ and $\mathbf{Q}(\mathbf{r})$ into Fourier series:

$$u(\mathbf{r}) = u_{\mathbf{0}} + u_{\mathbf{h}}\exp(i\mathbf{h}\cdot\mathbf{r}) + u_{-\mathbf{h}}\exp(-i\mathbf{h}\cdot\mathbf{r}) + \ldots,$$
$$\mathbf{Q}(\mathbf{r}) = \mathbf{Q_0} + \mathbf{Q_h}\exp(i\mathbf{h}\cdot\mathbf{r}) + \mathbf{Q_{-h}}\exp(-i\mathbf{h}\cdot\mathbf{r}) + \ldots.$$

We suppose that the crystal is magnetically saturated by an externally applied magnetic field $\mathbf{H}_a$. $\mathbf{Q_0}$ is then proportional to the macroscopic mean magnetic field $\mathbf{B} = \mu_0(\mathbf{M} + \mathbf{H}_a + \mathbf{H}_d)$, where $\mathbf{M}$ is the magnetization vector and $\mathbf{H}_d$ is the demagnetizing field. The results of Section 5.3.3.2 show that $\mathbf{Q_h}$ and $\mathbf{Q_{-h}}$ are proportional to the projection of $\mathbf{M}$ on the reflecting plane.

The four coefficients D_0, D_h, E_0 and E_h of (5.3.3.9) are found to satisfy a system of four homogeneous linear equations. The condition that the associated determinant has to be equal to 0 defines the dispersion surface, which is of order 4 and has four branches. An incident plane wave thus excites a system of four wavefields of the form of (5.3.3.9), generally polarized in various directions. A particular example of a dispersion surface, having an unusual shape, is shown in Fig. 5.3.3.1.

This is a much more complicated situation than in the case of non-magnetic crystals, in which one only needs to consider scalar wavefunctions which depend on two coefficients, such as D_0 and D_h, and which are related to hyperbolic dispersion surfaces of order 2, as fully described in Chapter 5.1 on X-ray diffraction.

In fact, all neutron experiments related to dynamical effects in diffraction by magnetic crystals have been performed under such conditions that the magnetization vector in the crystal is perpendicular to the diffraction vector **h**. In this case, the vectors $\mathbf{Q_h}$ and $\mathbf{Q_{-h}}$ are parallel or antiparallel to the vector $\mathbf{Q_0}$ which is chosen as the spin-quantization axis. The matrices $\boldsymbol{\sigma}\cdot\mathbf{Q_0}$, $\boldsymbol{\sigma}\cdot\mathbf{Q_h}$ and $\boldsymbol{\sigma}\cdot\mathbf{Q_{-h}}$ are then all diagonal matrices, and we obtain for the two spin states ($\pm$) separate dynamical equations which are similar to the dynamical equations for the scalar case, but with different structure factors, which are either the sum or the difference of the nuclear structure factor F_N and of the magnetic structure factor F_M:

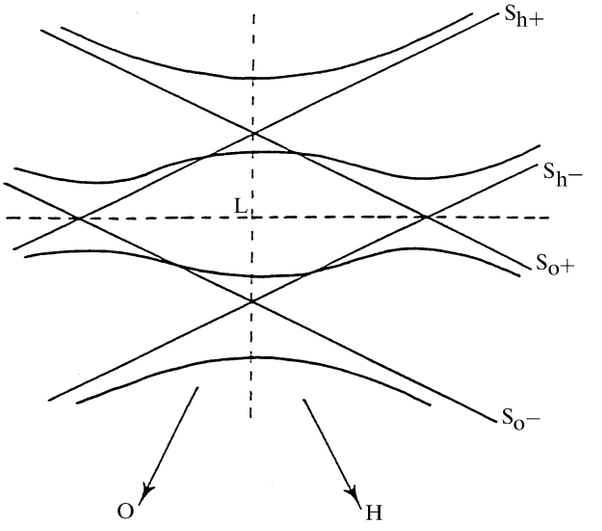

Fig. 5.3.3.1. Schematic plot of the two-beam dispersion surface in the case of a purely magnetic reflection such that $\mathbf{Q_h} = \mathbf{Q_{-h}} = \mathbf{Q_0}$ and that the angle between $\mathbf{Q_0}$ and $\mathbf{Q_h}$ is equal to $\pi/4$.

$$F_+ = F_N + F_M \text{ and } F_- = F_N - F_M. \qquad (5.3.3.11)$$

F_N and F_M are related to the scattering lengths of the ions in the unit cell of volume V_c:

$$F_N = V_c u_{\mathbf{h}} = \sum_i b_i \exp(-i\mathbf{h}\cdot\mathbf{r}_i);$$

$$F_M = V_c|\mathbf{Q_h}| = -\frac{\mu_0 m}{2h^2}\mu_n\boldsymbol{\sigma}\cdot\sum_i \boldsymbol{\mu}_{i\perp}(\mathbf{h}) f_i\left(\frac{\sin\theta}{\lambda}\right)\exp(-i\mathbf{h}\cdot\mathbf{r}_i).$$

The dispersion surface of order 4 degenerates into two hyperbolic dispersion surfaces, each of them corresponding to one of the polarization states ($\pm$). The asymptotes are different; this is related to different values of the refractive indices for neutron polarization parallel or antiparallel to $\mathbf{Q_0}$.

In some special cases the magnitudes of F_N and F_M happen to be equal. Only one polarization state is then reflected. Magnetic crystals with such a property (reflections 111 of the Heusler alloy Cu_2MnAl, or 200 of the alloy Co–8% Fe) are very useful as polarizing monochromators and as analysers of polarization.

If the scattering vector **h** is in the same direction as the magnetization, this reflection is a purely nuclear one (with no magnetic contribution), since F_M is then equal to 0. Purely magnetic reflections (without nuclear contribution) also exist if the magnetic structure involves several sublattices.

If **h** is neither perpendicular to the average magnetization nor in the same direction, the presence of non-diagonal matrices in the dynamical equations cannot be avoided. The dynamical theory of diffraction by perfect magnetic crystals then takes the complicated form already mentioned.

Theoretical discussions of this complicated case of dynamical diffraction have been given by Stassis & Oberteuffer (1974), Mendiratta & Blume (1976), Sivardière (1975), Belyakov & Bokun (1975, 1976), Schmidt *et al.* (1975), Bokun (1979), Guigay & Schlenker (1979*a*,*b*), and Schmidt (1983). However, to our knowledge, only limited experimental work has been carried out

on this subject. Successful experiments could only be performed for the simpler cases mentioned above.

5.3.3.4. *The dynamical theory in the case of perfect collinear antiferromagnetic crystals*

In this case, there is no average magnetization ($\mathbf{Q_0} = 0$). It is then convenient to choose the quantization axis in the direction of $\mathbf{Q_h}$ and $\mathbf{Q_{-h}}$. The dispersion surface degenerates into two hyperbolic surfaces corresponding to each polarization state along this direction for any orientation of the diffraction vector relative to the direction of the magnetic moments of the sublattices. These two hyperbolic dispersion surfaces have the same asymptotes. Furthermore, in the case of a purely magnetic reflection, they are identical.

The possibility of observing a precession of the neutron polarization in the presence of diffraction, in spite of the fact that there is no average magnetization, has been pointed out by Baryshevskii (1976).

5.3.3.5. *The flipping ratio*

In polarized neutron diffraction by a magnetically saturated magnetic sample, it is usual to measure the ratio of the reflected intensities I_+ and I_- measured when the incident beam is polarized parallel or antiparallel to the magnetization in the sample. This ratio is called the flipping ratio,

$$R = I_+/I_-, \tag{5.3.3.12}$$

because its measurement involves flipping the incident-beam polarization to the opposite direction. This is an experimentally well defined quantity, because it is independent of a number of parameters such as the intensity of the incident beam, the temperature factor or the coefficient of absorption. In the case of an ideally imperfect crystal, we obtain from the kinematical expressions of the integrated reflectivities

$$R_{\rm kin}(\mathbf{h}) = (I_+/I_-)_{\rm kin} = \left(\frac{|F_N + F_M|}{|F_N - F_M|}\right)^2. \tag{5.3.3.13}$$

In the case of an ideally perfect thick crystal, we obtain from the dynamical expressions of the integrated reflectivities

$$R_{\rm dyn}(\mathbf{h}) = (I_+/I_-)_{\rm dyn} = \frac{|F_N + F_M|}{|F_N - F_M|}. \tag{5.3.3.14}$$

In general, $R_{\rm dyn}$ depends on the wavelength and on the crystal thickness; these dependences disappear, as seen from (5.3.3.14), if the path length in the crystal is much larger than the extinction distances for the two polarization states. It is clear that the determination of $R_{\rm kin}$ or $R_{\rm dyn}$ allows the determination of the ratio F_M/F_N, hence of F_M if F_N is known. In fact, because real crystals are neither ideally imperfect nor ideally perfect, one usually introduces an extinction factor y (extinction is discussed below, in Section 5.3.4) in order to distinguish the real crystal reflectivity from the reflectivity of the ideally imperfect crystal. Different extinction coefficients y_+ and y_- are actually expected for the two polarization states. This obviously complicates the task of the determination of F_M/F_N.

In the kinematical approximation, the flipping ratio does not depend on the wavelength, in contrast to dynamical calculations for hypothetically perfect crystals (especially for the Laue case of diffraction). Therefore, an experimental investigation of the wavelength dependence of the flipping ratio is a convenient test for the presence of extinction. Measurements of the flipping ratio have been used by Bonnet *et al.* (1976) and by Kulda *et al.* (1991) in order to test extinction models. Baruchel *et al.* (1986) have compared nuclear and magnetic extinction in a crystal of MnP.

Instead of considering only the ratio of the integrated reflectivities, it is also possible to record the flipping ratio as a function of the angular position of the crystal as it is rotated across the Bragg position. Extinction is expected to be maximum at the peak and the ratio measured on the tails of the rocking curve may approach the kinematical value. It has been found experimentally that this expectation is not of general validity, as discussed by Chakravarthy & Madhav Rao (1980). It would be valid in the case of a perfect crystal, hence in the case of pure primary extinction. It would also be valid in the case of secondary extinction of type I, but not in the case of secondary extinction of type II [following Zachariasen (1967), type II corresponds to mosaic crystals such that the diffraction pattern from each block is wider than the mosaic statistical distribution].

5.3.4. Extinction in neutron diffraction (non-magnetic case)

The kinematical approximation, which corresponds to the first Born approximation in scattering theory, supposes that each incident neutron can be scattered only once and therefore neglects the possibility that the neutrons may be scattered several times. Because this is a simple approximation which overestimates the crystal reflectivity, the actual reduction of reflectivity, as compared to its kinematical value, is termed *extinction.* This is actually a typical dynamical effect, since it is a multiple-scattering effect.

Extinction effects can be safely neglected in the case of scattering by very small crystals; more precisely, this is possible when the path length of the neutron beam in the crystal is much smaller than $\Delta = V_c/\lambda F$, where λ is the neutron wavelength and F/V_c is the scattering length per unit volume for the reflection considered. Δ is sometimes called the 'extinction distance'.

A very important fact is that extinction effects also vanish if the crystal is imperfect enough, because each plane-wave component of the incident beam can then be Bragg-reflected in only a small volume of the sample. This is the extinction-free case of 'ideally imperfect crystals'. Conversely, extinction is maximum (smallest value of y) in the case of ideally perfect non-absorbing crystals.

Clearly, no significant extinction effects are expected if the crystal is thick but strongly absorbing, more precisely if the linear absorption coefficient μ is such that $\mu\Delta \gg 1$. Neutron diffraction usually corresponds to the opposite case ($\mu\Delta \ll 1$), in which extinction effects in nearly perfect crystals dominate absorption effects.

Extinction effects are usually described in the frame of the mosaic model, in which the crystal is considered as a juxtaposition of perfect blocks with different orientations. The relevance of this model to the case of neutron diffraction was first considered by Bacon & Lowde (1948). If the mosaic blocks are big enough there is extinction within each block; this is called *primary extinction.* Multiple scattering can also occur in different blocks if their misorientation is small enough. In this case, which is called *secondary extinction*, there is no phase coherence between the scattering events in the different blocks. The fact that empirical intensity-coupling equations are used in this case is based on this phase incoherence.

In the general case, primary and secondary extinction effects coexist. Pure secondary extinction occurs in the case of a mosaic crystal made of very small blocks. Pure primary extinction is observed in diffraction by perfect crystals.

The parameters of the mosaic model are the average size of the perfect blocks and the angular width of their misorientation distribution. The extinction theory of the mosaic model provides a relation between these parameters and the extinction coefficient,

references